Discovery and Characterization of a Photo-Oxidative Histidine-Histidine Cross-Link in IgG1 Antibody Utilizing ^{18}O-Labeling and Mass Spectrometry

Min Liu,[*,†,§] Zhongqi Zhang,[‡] Janet Cheetham,[†] Da Ren,[*,‡] and Zhaohui Sunny Zhou[*,§]

[†]Analytical Research and Development, Amgen, One Amgen Center Drive, Thousand Oaks, California 91320, United States

[‡]Process and Product Development, Amgen, One Amgen Center Drive, Thousand Oaks, California 91320, United States

[§]Barnett Institute of Chemical and Biological Analysis, Department of Chemistry and Chemical Biology, Northeastern University, 360 Huntington Avenue, Boston, Massachusetts 02115, United States

S *Supporting Information*

ABSTRACT: A novel photo-oxidative cross-linking between two histidines (His-His) has been discovered and characterized in an IgG1 antibody via the workflow of XChem-Finder, ^{18}O labeling and mass spectrometry (*Anal. Chem.* 2013, 85, 5900−5908). Its structure was elucidated by peptide mapping with multiple proteases with various specificities (e.g., trypsin, Asp-N, and GluC combined with trypsin or Asp-N) and mass spectrometry with complementary fragmentation modes (e.g., collision-induced dissociation (CID) and electron-transfer dissociation (ETD)). Our data indicated that cross-linking occurred across two identical conserved histidine residues on two separate heavy chains in the hinge region, which is highly flexible and solvent accessible. On the basis of model studies with short peptides, it has been proposed that singlet oxygen reacts with the histidyl imidazole ring to form an endoperoxide and then converted to the 2-oxo-histidine (2-oxo-His) and His+32 intermediates, the latter is subject to a nucleophilic attack by the unmodified histidine; and finally, elimination of a water molecule leads to the final adduct with a net mass increase of 14 Da. Our findings are consistent with this mechanism. Successful discovery of cross-linked His-His again demonstrates the broad applicability and utility of our XChem-Finder approach in the discovery and elucidation of protein cross-linking, particularly without *a priori* knowledge of the chemical nature and site of cross-linking.
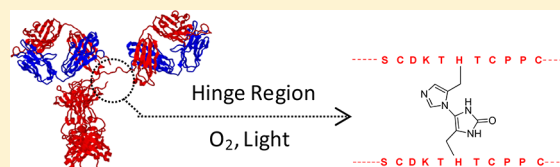
Protein cross-links are ubiquitous in biological systems and biopharmaceuticals. They are also involved in disease pathologies such as Alzheimer[1−3] and cataractogenesis.[2,4] As one of the post-translational modifications and degradations that occur during biopharmaceutical protein production processing and storage, cross-links have been reported to result in aggregation, loss of bioactivity, and immunogenicity.[5−7]

Despite the rapid advancements in mass spectrometry and data analysis algorithms, characterization of protein cross-links remains challenging due to their structural complexity.[8] Whereas a limited set of cross-linked structures (e.g., thioether[7,9−12]) have been characterized, most remain unknown; for example, the nondisulfide covalent cross-linking in crystalline,[4,13,14] collagen,[15] ubiquitylated proteins,[3] ribonuclease A,[16] and monoclonal antibodies.[17,18] It is particularly challenging to characterize protein cross-linking without prior knowledge of the chemical nature and sites of cross-linking as no theoretical mass or spectrum can be predicted. In contrast, numerous chemical cross-links with well-established cross-linking chemistry have been used in the investigation of protein structures and protein−protein interactions.[19−25] Since predefined cross-linking chemistry is involved, various specialized algorithms have been developed for data analysis for each incorporated cross-link. Naturally, these approaches are less amenable to the

identification of cross-links with undefined cross-linking chemistry. Recently, we developed a workflow, XChem-Finder, that is generally applicable for protein cross-linking. It involves, first, the detection of cross-linked peptides via the unique isotope patterns imparted by ^{18}O-labeling of their two termini (in comparison, one terminus for a linear peptide), and then integrated mass spectrometric and data analysis.[8]

IgG1 and IgG2 are the most popular therapeutic monoclonal antibodies on the market.[26] Applying our XChem-Finder workflow, we have discovered and characterized a novel histidine-histidine (His-His) cross-link in IgG1 antibody. High molecular weight species in the light-irradiated IgG1 were detected by reduced SDS-PAGE and size exclusion chromatography (SEC). Our LC−MS analysis indicated that cross-linking occurred across two identical conserved histidine residues (His220) on two separate heavy chains in the hinge region, which is highly flexible and solvent accessible. The cross-linking chemistry is consistent with the proposed mechanism based on model peptides under photo-oxidative conditions (see Scheme 1).[16,27−29] Successful discovery of the His-His cross-link in IgG1

Scheme 1. Proposed Mechanism for the Formation of His-His Crosslink via Photo-Oxidation Intermediates
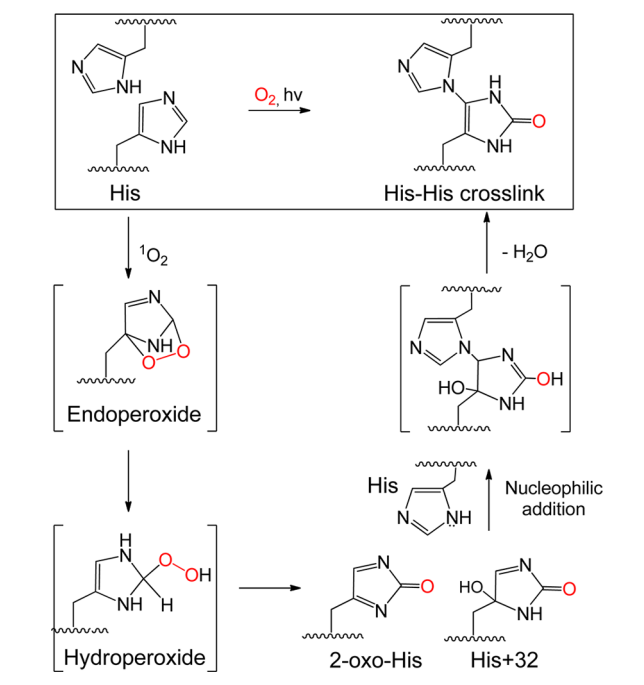
has further demonstrated the general applicability and power of our XChem-Finder workflow. To the best of our knowledge, our work reported herein is the first example of such cross-linking in a protein.

◼ EXPERIMENTAL SECTION

Chemicals. All chemicals were reagent grade or above. Guanidine hydrochloride (GndHCl), ethylenediaminetetraacetic acid (EDTA), dithiothreitol (DTT), iodoacetic acid (IAA), trifluoroacetic acid (TFA), acetonitrile (ACN), HPLC-grade water, and bradykinin were from Sigma-Aldrich (St. Louis, MO). Sequencing grade trypsin, GluC, and Asp-N were from Roche (Indianapolis, IN). ^{18}O-water (97%) was from Cambridge Isotope Laboratories (Andover, MA). Recombinant monoclonal IgG1 antibody (antistreptavidin immunoglobulin gamma 1) was produced in Chinese hamster ovary (CHO) cells (Amgen, Thousand Oaks, CA), purified according to standard manufacturing procedures, formulated at a concentration of 30 mg/mL in 50 mM sodium acetate at pH 5.2, and stored at −70 °C.

Generation of Stressed Sample. After being exchanged into various buffers of biopharmaceutical interest (50 mM sodium acetate at pH 4.8, 50 mM sodium phosphate at pH 7.4, 50 mM sodium bicarbonate at pH 9.0 or water), the IgG1 antibody at a concentration of 5 mg/mL in a clear 3 mL glass vial was put into a light chamber (Atlas Suntest CPS+ with Xenon Lamp and ID65 solar filter, controlled irradiance at 300−800 nm, light intensity at 765 W/m²) and exposed to light irradiation for 7, 14, and 22 h. These conditions represent the light irradiance of 1×, 2×, and 3× ICH (International Conference on Harmonization of Technical Requirements for Registration of Pharmaceuticals for Human Use), respectively.

Aggregates by Size Exclusion Chromatography. Size exclusion chromatography (SEC) analysis for reduced IgG was carried out as described.[30] Briefly, IgG1 was diluted to 1 mg/mL in a denaturing buffer (7.5 M Gnd-HCl, 2 mM EDTA and 0.25 M Tris-HCl, pH 7.5) at room temperature. Reduction was

accomplished by 10 mM DTT at room temperature for 30 min. Then 50 μL of the above samples was injected onto a TSKgel G3000 SW$_{XL}$ column (7.8 mm × 300 mm, 5 μm) with an isocratic mobile phase of 0.1% TFA/H$_2$O−ACN (80:20) and a flow rate of 0.2 mL/min. The column was set at room temperature, and the UV detector was at 280 nm.

Reduction, Alkylation, Tryptic Digestion and ^{18}O-Labeling of IgG1. IgG1 was digested by trypsin similarly to the procedure described by Ren et al.[31] Briefly, IgG1 was diluted to 1 mg/mL in a denaturing buffer (7.5 M GndHCl, 2 mM EDTA, and 0.25 M Tris-HCl, pH 7.5) to a final volume of 0.5 mL. Reduction was accomplished with the addition of 3 μL of 0.5 M DTT followed by 30 min incubation at room temperature. S-Carboxymethylation was achieved with the addition of 7 μL of 0.5 M IAA, and the resulting mixture was incubated at room temperature in the dark for 15 min. Excess IAA was quenched with the addition of 4 μL of 0.5 M DTT. The reduced and alkylated IgG1 samples were subsequently exchanged into the digestion buffer (0.1 M Tris-HCl at pH 7.5) using a NAP-5 size-exclusion column (GE Healthcare, Piscataway, NJ). Next, two aliquots (200 μL each) were completely dried via SpeedVac and reconstituted separately into the same volume of ^{18}O-water or ^{16}O-water; then 6 μL of 1 mg/mL trypsin in ^{18}O-water or ^{16}O-water solution, respectively, was added to achieve a 1:25 (w/w) enzyme/substrate ratio. The reaction mixtures were incubated at 37 °C for 30 min.

Other proteolytic digestions of IgG1 (Asp-N, Trypsin combined with GluC, and Asp-N combined with GluC) were performed in ^{16}O-water only. Proteases were added to 100 μL of the above buffer-exchanged antibody to achieve a 1:25 (w/w) enzyme/substrate ratio. The reaction mixtures were incubated at 37 °C overnight.

Limited Asp-N digestion was performed by adding 6 μg of Asp-N into a 300 μL digest (of trypsin combined with GluC) and incubating at 37 °C for 1.5 h for LC/CID-MS analysis. An aliquot of 200 μL of the above digest was dried via SpeedVac and reconstituted into 40 μL of water for LC/ETD-MS analysis.

RP-HPLC. The proteolytic digests of IgG1 (25 μL) were separated on a Jupiter C5 column (250 mm × 2.0 mm, 5 μm, 300 Å, Phenomenex, Torrance, CA) at 50 °C with a flow rate of 200 μL/min on a HPLC system (Agilent 1100, Palo Alto, CA). Mobile phase A was 0.1% TFA in water (v/v), while mobile phase B contained 0.085% TFA in 90% ACN/10% water. A gradient was applied by holding at 2% B for 2 min, increasing to 22% B in 38 min, then 42% B in 80 min, then 100% B in 25 min followed by holding at 100% B for 5 min. The column was re-equilibrated at 2% B for 30 min prior to next injection.

For ETD analysis, digests of IgG1 (6 μL) were separated on a PROTO C4 column (150 mm × 1.0 mm, 5 μm, 300 Å, Higgins Analytical, Mountain View, CA) at 50 °C with a flow rate of 60 μL/min on a HPLC system (Agilent 1100, Palo Alto, CA). Mobile phase A was 0.1% FA/0.02% TFA in water (v/v) while mobile phase B contained 0.1% FA/0.02% TFA in 90% ACN/10% water. The same gradient as described above was applied.

Mass Spectrometry. An LTQ-Orbitrap mass spectrometer (Thermo Fisher Scientific, San Jose, CA) was used in-line with a HPLC system for the analyses of the IgG1 proteolytic digests. A full MS scan (with 60 000 resolution at m/z 400 and an automatic gain control (AGC) target value of 2 × 10⁵) followed by data-dependent MS/MS scans of the three most abundant precursor ions was set up to acquire both the peptide mass and sequence information. The spray voltage was 5.5 kV, and the capillary temperature was 250 °C. The instrument was tuned
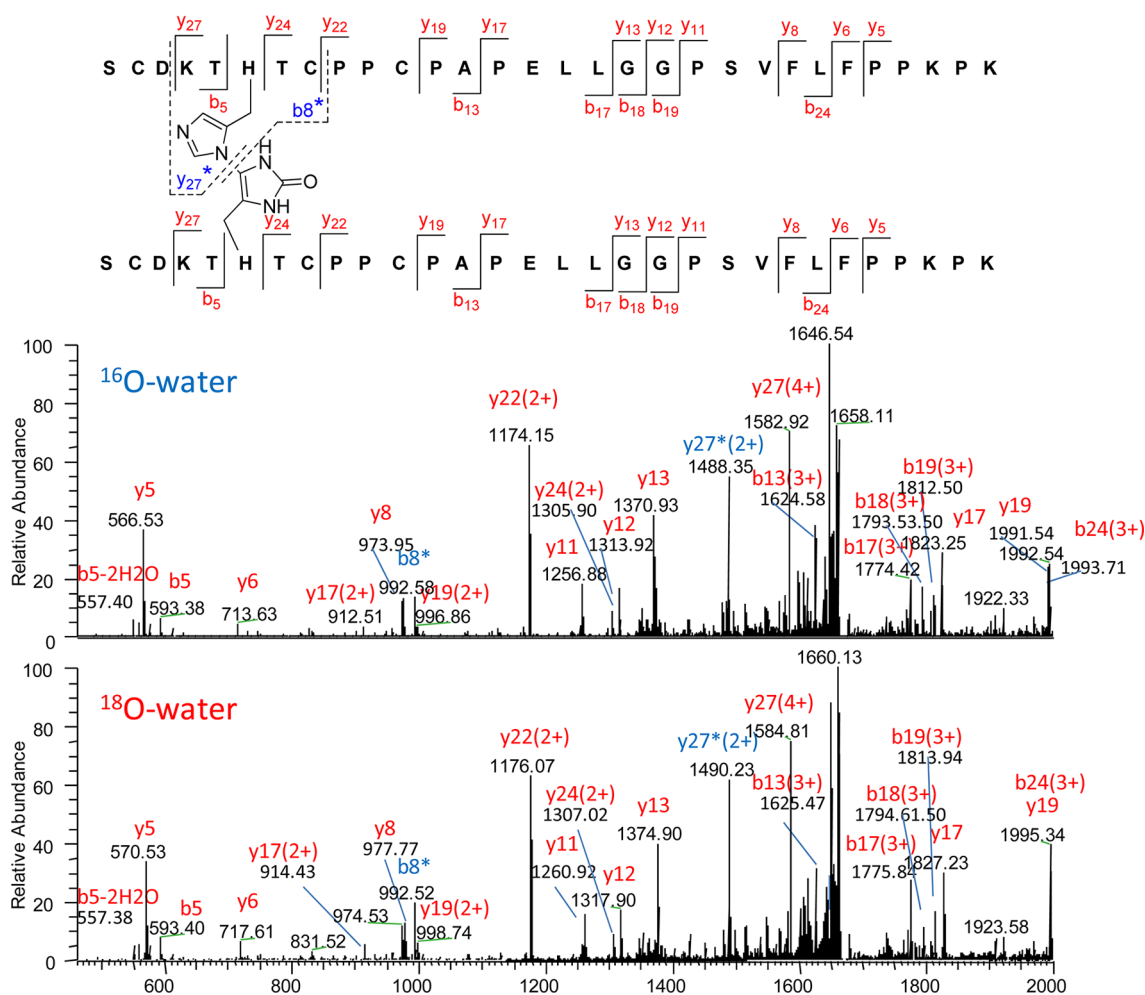
Figure 1. CID MS/MS spectra of the quadruply charged precursor ions m/z 1673.54 (^{16}O-labeled C-termini) and 1675.54 (^{18}O-labeled C-termini) of the cross-linked tryptic peptide S215−K244/S215−K244. Characteristic mass shift imparted by the heavier isotope ^{18}O was observed (e.g., the mass shift of 4 Da for y5 ions in ^{16}O- vs ^{18}O-water, 566.53 vs 570.53). The y27* ion results from cleavage of the His-His bond while the y27 ion contains the cross-linking site. MS3 spectrum of the y27* ion (m/z 1488.35) is shown in Figure S2-3 in the Supporting Information.

using the doubly charged ion of a synthetic peptide, bradykinin. The MS/MS spectra were obtained using CID with a normalized collision energy of 35%. For MS/MS with ion detection in the Orbitrap, the AGC target was set to 3×10^6, resolution to 7 500, and the precursor isolation width to 4 m/z unit. Under our experimental conditions, the typical mass accuracy in full MS scan and FT MS/MS is 5 and 10 ppm, respectively.

ETD spectra were acquired on a Thermo-Scientific LXQ-XL mass spectrometer in centroid mode with an isolation width of 5, reaction time of 75 ms, and reagent target value of 1×10^5, using singly charged fluoranthene anions as the ETD reagent. Both CID and ETD data were analyzed for peptide identification, using a custom-written algorithm MassAnalyzer and verified manually.[32−35]

RESULTS AND DISCUSSION

A novel His-His cross-link in proteins has been discovered via our XChem-Finder workflow, without predefined cross-linking chemistry. Peptide mapping with mass spectrometry has established that the cross-link occurred across two identical His220 on each of the two heavy chains in the hinge region.

Detection of Cross-Linked Protein. Photoinduced non-reducible high molecular weight species were detected by reducing SDS-PAGE; their intensities increased with longer light

exposure (Figure S1A in the Supporting Information). Their formation was pH-dependent: less favorable under acidic conditions, such as pH ∼5 for typical formulation of proteins (Figure S1B in the Supporting Information), and more favorable in neutral or basic buffers that are commonly used in protein production and purification (Figure S1B in the Supporting Information). The cross-linked species were also quantified by size exclusion chromatography (SEC) (Figure S1C, D in the Supporting Information). Mobile phase of 0.1% TFA/H$_2$O− ACN (80:20) was used to avoid hydrophobic interaction with the stationary phase.[30] The results from SEC and SDS-PAGE were consistent. The total amounts of the early elution peaks observed were at the level of 0.2, 4.5, 9.5, and 16.5% by peak area in the control sample and samples exposed to 1×, 2×, 3× ICH irradiation, respectively (Figure S1C in the Supporting Information). The cross-links were also observed to increase to 25.8% in 50 mM NaHCO$_3$ pH 9.0, 15.7% in 50 mM sodium phosphate pH 7.4, and 6.3% in 50 mM sodium acetate pH 4.8. It is interesting to note that the control sample (without light stress) already contained small yet detectable amount of cross-linking (0.4%, Figure S1D in the Supporting Information), suggesting such modifications could occur during routine protein production and process. The chemical nature and site of cross-

Table 1. Crosslinked Peptides Obtained from Digestion of IgG1 by Various Proteases and the Combination Thereof[a]

Name	Proteases	Crosslinked Peptides	RT (min)	m/z (Charge)	Obs. Mass (Da)	Theor. Mass (Da)	Mass Error (ppm)
S215-K244/ S215-K244	Trypsin	(K)²¹⁵SCDKT**H**TCPPCPAPELLGGPSVFLFPPKPK²⁴⁴(D) (K)²¹⁵SCDKT**H**TCPPCPAPELLGGPSVFLFPPKPK²⁴⁴(D)	112.48	1673.54 (4+)	6687.149	6687.153	0.6
D217-K244/ D217-K244	Asp-N	(C)²¹⁷DKT**H**TCPPCPAPELLGGPSVFLFPPKPK²⁴⁴(D) (C)²¹⁷DKT**H**TCPPCPAPELLGGPSVFLFPPKPK²⁴⁴(D)	113.07	1549.53 (4+)	6191.064	6191.060	0.6
S215-E229/ S215-E229	Trypsin + GluC	(K)²¹⁵SCDKT**H**TCPPCPAPE²²⁹(L) (K)²¹⁵SCDKT**H**TCPPCPAPE²²⁹(L)	41.19	1178.77 (3+)	3531.289	3531.286	0.6
D217-E229/ D217-E229	Asp-N + GluC	(C)²¹⁷DKT**H**TCPPCPAPE²²⁹(L) (C)²¹⁷DKT**H**TCPPCPAPE²²⁹(L)	40.53	1013.41 (3+)	3035.193	3035.193	0.0
D217-E229/ S215-E229	Trypsin + GluC; then Asp-N	(C)²¹⁷DKT**H**TCPPCPAPE²²⁹(L) (K)²¹⁵SCDKT**H**TCPPCPAPE²²⁹(L)	40.31	1096.09 (3+)	3283.234	3283.240	1.9

[a]The crosslinking sites are labeled in red and bold. All cysteines are alkylated with IAA. Peptides are shown with the amino acid residue position in IgG1 in superscript and the adjoining amino acid residues before cleavage in parentheses.

linking was discovered by our XChem-Finder workflow as detailed next.[8]

Detection of Cross-Linked Peptide. Tryptic digestion in ^{18}O-water results in the incorporation of two [18]O atoms in each of the newly generated C-termini;[36,37] hence, two [18]O atoms for a linear tryptic peptide (with one C-terminus) and four [18]O atoms for a cross-linked peptide (with two C-termini).[38−40] As shown in Figure S2-1 in the Supporting Information, the isotopic distribution of the peptide at m/z 1673.54 (quadruply charged, monoisotopic mass 6687.149 Da) shows a mass shift of 8 Da (i.e., four ^{18}O) in ^{18}O-water compared to that from ^{16}O-water, indicating it contains two C-termini and is a cross-linked peptide.

Elucidation of Cross-Linking Chemistry. The cross-linked peptide m/z 1673.54 underwent FT MS/MS analysis. As described in our previous paper,[8] the fragment ions obtained were searched against the amino acid sequence of the IgG1 via FindPept to match all possible peptide fragments, see Table S1 in the Supporting Information. On the basis of the peptide ladders observed, a partial sequence K218−K244 (KTHTCPPCPAPEL-LGGPSVFLFPPKPK, see Table S1 in the Supporting Information) was identified. Then, the partial sequence was extended to a putative full-length tryptic peptide S215−K244 (SCDKTHTCPPCPAPELLGGPSVFLFPPKPK, 3336.587 Da). Since the fragment ions only matched this single peptide, we surmised that cross-linking occurred across the two identical peptides. The combined mass of the two unmodified (native) peptides is 6673.174 Da, which also satisfies the mass limitation conferred by the observed mass of the cross-linked peptide (6687.149 Da, see Table S2 in the Supporting Information).

In order to elucidate the cross-linking chemistry, elemental composition analysis of the cross-link was performed as illustrated in Table S2 in the Supporting Information. The mass difference between the sum of the two native peptide chains and observed mass of the cross-linked peptide is 13.975 Da, for which three potential formula (O−2H, N, or CH_2) were proposed. From a chemistry perspective, it is difficult to add just one nitrogen atom or a CH_2 group. On the other hand, addition of one oxygen atom coupled with the loss of two hydrogen atoms (O−2H) indicates oxidation. The putative peptide chain K218−K244 contains His, of which oxidation and cross-linking have been reported.[28,29] In addition, the formula O−2H gives the

lowest mass error (0.004 Da). Therefore, a potential His-His cross-linking structure is proposed as illustrated in Table S2 in the Supporting Information and Figure 1 and verified as described next.

Structural Confirmation by Mass Spectrometry. First, the calculated mass of the His-His cross-linked peptide (6687.153 Da) is in good agreement with the observed mass (6687.149 Da, mass error 0.6 ppm, see Table 1). Second, the series of b- and y-ions are highly consistent with the proposed structure (Figure 1). The observed y-ions from y5 to y24 and the b5 ions correspond to fragment ions with no cross-linking site, while the y-ions from y27 and the b-ions from b13 to b24 are from fragments that contain the cross-linked histidine residues. These data support cross-linking at His 220. Moreover, y27* ion (in blue) and b8* ion (in blue) are peptide fragments resulting from cleaving the bond connecting the two cross-linked histidine residues (see Figure 1). The missed cleavage by trypsin at Lys218 is likely due to its close proximity to the cross-linking site at His220, reminiscent of similarly missed cleavages in the case of thioether cross-linking.[9] The second missed cleavage at Lys242 is likely due to the presence of adjacent proline residues. The two missed tryptic cleavages in the cross-linked peptide would have been especially challenging to handle by traditional database-dependent algorithms, again highlighting the utility of our XChem-Finder workflow.[8,41,42]

Additional Confirmation by ^{18}O/^{16}O-Isotope Fragment Ions Pattern. Since the fragment ions containing no (zero), one, or two C-termini of the cross-linked peptides displayed a mass shift of 0, 4, and 8 Da, respectively, in the corresponding MS/MS spectra obtained from [18]O- and ^{16}O-water, the examination of mass shift of fragment ions can lend further support for the assignment of fragment ions. For example, as shown in Figure 1, b-ions prior to the cross-linking site (e.g., b5) have no mass shift between the ^{18}O-water and ^{16}O-water digests. On the other hand, the y-ions without the cross-linking site (e.g., y5) gave a mass shift of 4 Da. All assignments were verified by their distinct mass shift in ^{18}O, depending on the number of C-termini they contain.

Additional Confirmation by MS³ Analysis. Several abundant fragment ions shown in Figure 1 were selected for MS³ analysis which simplified and further confirmed data
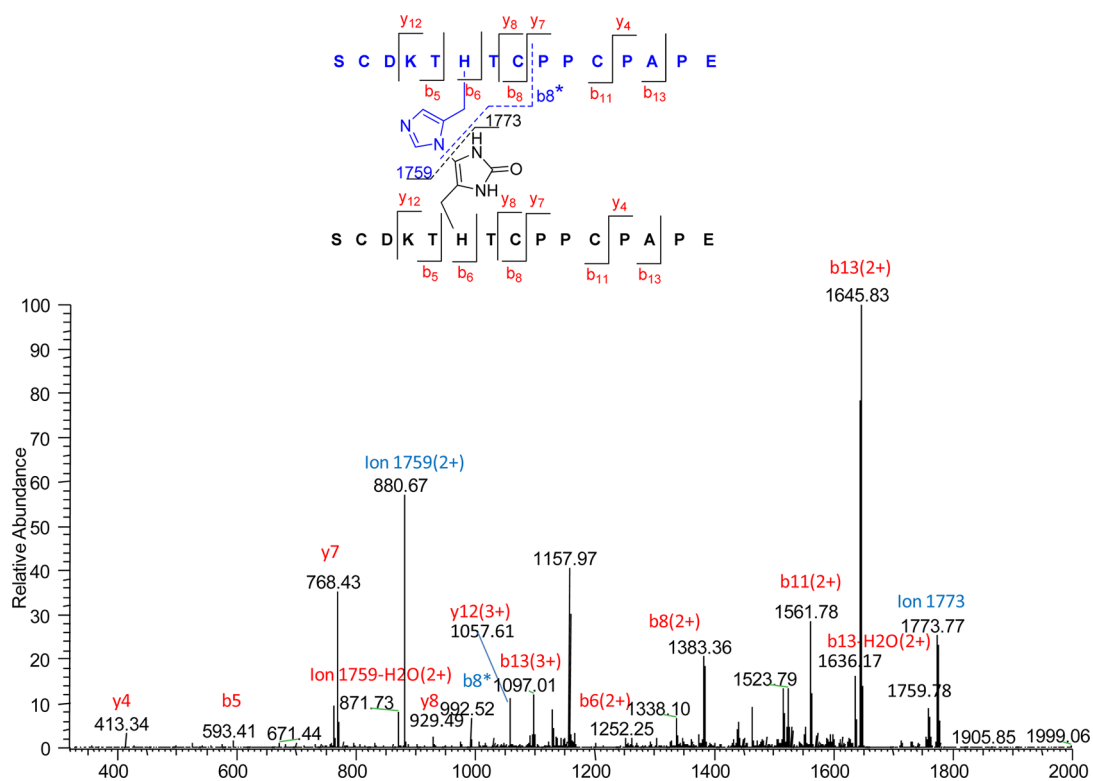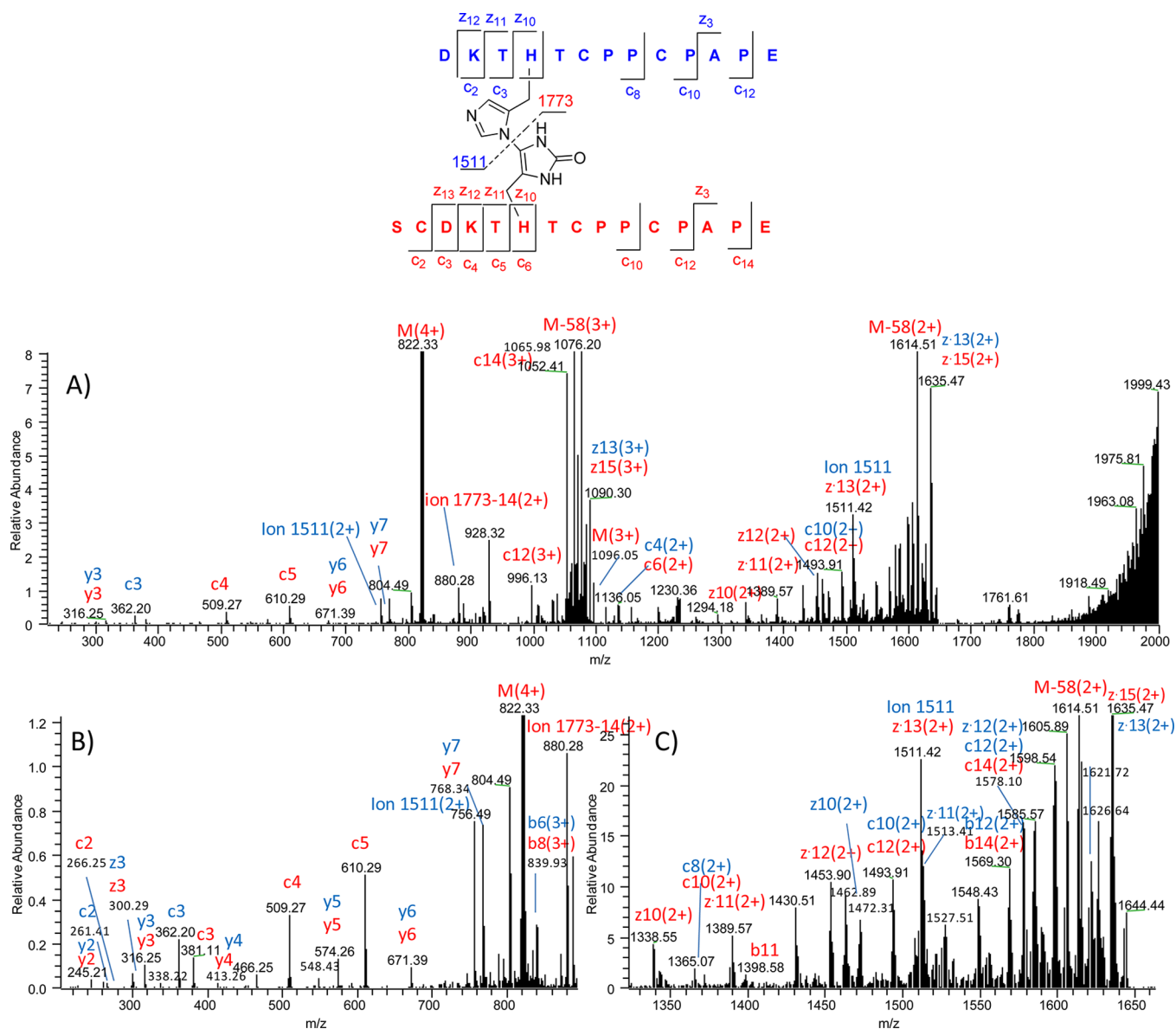
Figure 2. CID MS/MS spectrum of the triply charged precursor ion m/z 1178.77 of the cross-linked S215-E229/S215-E229 peptide generated from combined trypsin and GluC digestion. The b8* ion results from cleavage of the His-His bond while the b8 ion contains the cross-linking site.
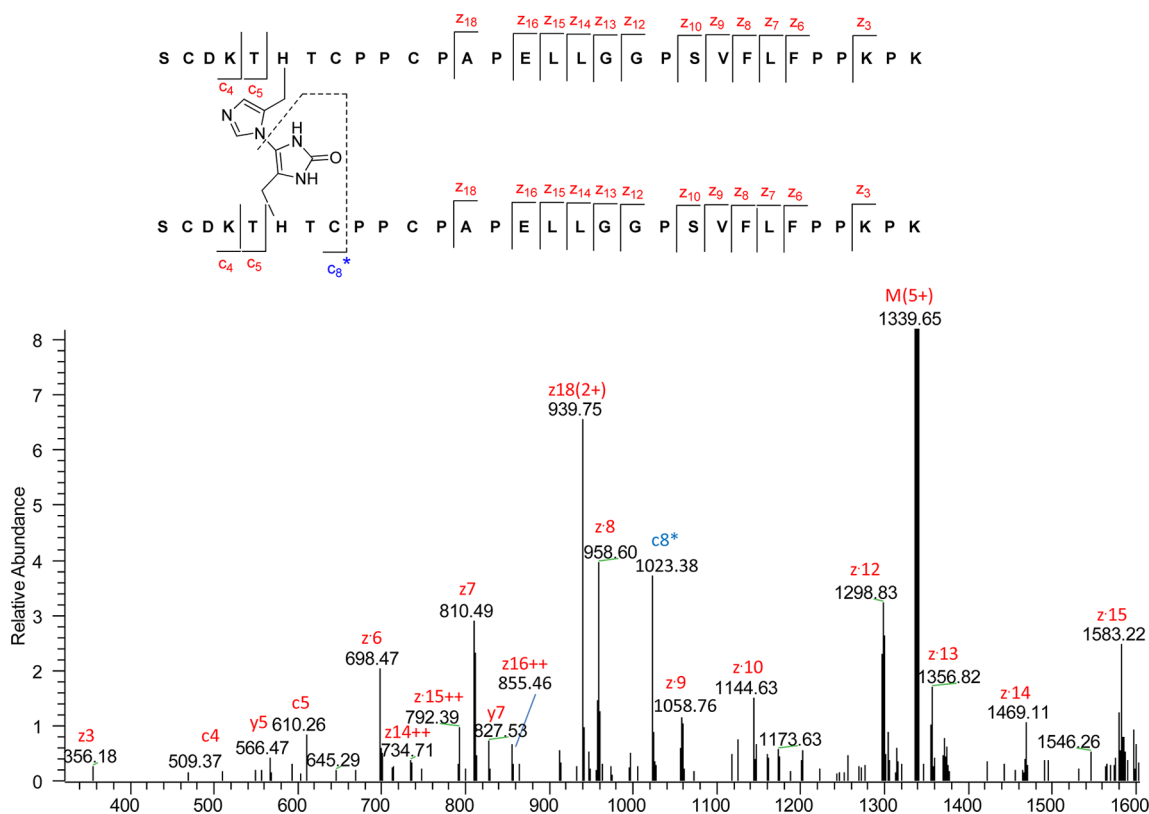
Figure 3. ETD MS/MS spectrum of the precursor ion m/z 1339.70 ($z = 5$) of the cross-linked tryptic peptide S215−K244/S215−K244.

interpretation. For example the fragment ion m/z 1488.35 shown in Figure 1 could not be assigned initially, so it was selected for MS[3] analysis (Figure S2-3 in the Supporting Information). The

analysis established that it was the y27* ion (in blue) generated from cleaving the bond connecting the two cross-linked histidine residues.

Figure 4. ETD MS/MS spectrum of the quadruply charged precursor ion m/z 821.09 of the cross-linked peptide D217−E229/S215−E229 generated by limited Asp-N digestion of fully digested IgG1 by trypsin and GluC.

Peptide Mapping with Multiple Proteases. Since this is the first report of His-His cross-linking in a protein, peptide mapping with additional proteases was carried out to glean complementary data.[43,44] In additional to trypsin, proteases with different sequence specificity (e.g., Asp-N[45−47] or GluC[48]) and combined proteases (e.g., trypsin with GluC, and Asp-N with GluC) were employed. Additional cross-linked peptides containing His220 were detected and analyzed: D217-K224/D217-K224 from Asp-N, S215-E229/S215-E229 from trypsin with GluC, and D217-E229/D217-E229 from Asp-N and GluC, respectively. In each case, the observed mass was in good agreement with its theoretical mass with mass errors ranging from 0.0 to 0.6 ppm (see Table 1). The y- and b-ions were also consistent with the corresponding structure (Figure 2 and Figures S3-1 and S5-1 in the Supporting Information). Similar to the tryptic peptide, the cross-linking site and chemistry were further supported by the presence of several ions generated from cleaving the bond connecting the two cross-linked histidine residues, such as the doubly charged ion at m/z 880.67, the singly

charged ion at m/z 1773.77, and the singly charged ion at m/z 992.52 (b8*) shown in Figure 2 (all highlighted in blue).

ETD MS/MS Analysis. As an alternative fragmentation technique, ETD provides sequence information complementary to that obtained from CID by cleaving a peptide backbone in a less selective manner than CID.[34,49,50] Higher charge state ions usually generate more effective ETD fragmentation;[50] therefore, formic acid instead of TFA was used in the mobile phase to increase charge state for more effective ETD fragmentation and to minimize ion suppression. All ETD MS/MS spectra were collected with supplemental activation and dominated by charge reduced species. The charge states of 5, 6, 4, and 4 for the peptide S215−K244/S215−K244, D217−K244/D217−K244, S215−E229/S215−E229, and D217−E229/D217−E229, respectively, offered optimal ETD fragmentation for each cross-linked peptide (Figure 3 and Figures S3-2, S4, and S5-2 in the Supporting Information). While different than those from CID, the fragmentation patterns from ETD also support our proposed cross-linking site and chemistry. For instance, the c5 and c*8 ions

in Figure 3 narrow the site within the HTC motif; the c4 ion in Figure S3-2 in the Supporting Information, c5 and c6 ions in Figure S4 in the Supporting Information, and c3 and z8 ions in Figure S5-2 in the Supporting Information pinpointed the cross-link at His220.

Mechanism of Formation for His-His Cross-Link. Photo-oxidation and cross-linking between histidine residues have been studied using both free histidine and model peptides. The commonly accepted mechanism is depicted in Scheme 1. Singlet oxygen (e.g., generated from photoactivated dye rose bengal[51]) reacts with histidine to form a highly reactive and labile endoperoxide intermediate, which converts into a hydroperoxide intermediate and then 2-oxo-histidine (2-oxo-His) and His + 32 intermediates. Subsequently, the His + 32 intermediate can be attacked by the nucleophilic imidazole of another histidine residue, followed by the elimination of a water molecule to give the final cross-linking product (Scheme 1).[16,27−29,52,53] As discussed below, our results are consistent with this mechanism.

First, oxygen was present in all buffers and water in which IgG1 was exposed to light irradiation. Second, several photo-oxidation intermediates were observed. The endoperoxide intermediate is unstable and has only been observed by low-temperature NMR study,[16,27] so we are not surprised that it was not detected by our LC−MS analysis. However, the subsequent oxidation intermediates, 2-oxo-His (+14 Da) and His+32 species (+ 32 Da), were detected. The peptides with masses 14 and 32 Da greater than the unmodified peptide, S215−K244 (SCDKTHTCPPCP-APELLGGPSVFLFPPKPK), were observed in the light stressed samples but not in the control sample (Table S3 in the Supporting Information). Tandem mass spectra confirmed their structures to be the peptides modified at His220 (Figures S7-2 and S7-3 in the Supporting Information). Third, the reported model studies showed the cross-linking was favored at higher pH, as the neutral (deprotonated) imidazole in histidine ($pK_a \sim 6$) is more reactive for nucleophilic attack and thus results in a higher yield of cross-linking.[54] Similar pH dependence was observed in our case as discussed above (Figure S1 in the Supporting Information). Lastly, the two His220 residues are juxtaposed in the hinge region, which is highly exposed to solvent and flexible, as illustrated in Figure S8 in the Supporting Information. In fact, in most crystal structures, the side chains of residues in the hinge region could not be located, indicating a high degree of flexibility. In this illustrative structure (PDB 1HZH), the side chain of only one histidine residue was observed.

On the basis of the reaction pathway and protein structure, cross-linking of lysine with the oxidized histidine via nucleophilic addition is also plausible,[16,27] and Lys218 is in the vicinity of His220. Therefore, great effort was made to determine whether the cross-linking is His220-His220 or Lys218-His220. This is particularly challenging due to the pseudosymmetry in the cross-linked peptide; in other words, when the two chains share identical sequence (e.g., in Figures 1 and 2), any fragment ion could come from either one chain or both. For example, c4 and c5 ions in Figure 3 indicated the existence of unmodified Lys218 and Thr219 but could not unambiguously establish whether they were from one chain or both. To address this issue, an asymmetric cross-linked peptide (i.e., two chains of different length) was generated via limited digestion. IgG1 fully digested by trypsin and GluC was treated with Asp-N for a limited time to obtain a cross-linked peptide with two different chains D217−E229/S215−E229 (Figure 4 and Figure S6 in the Supporting Information). Its precursor ion m/z 1096.09 ($z = 3$) has an observed mass of 3283.234 Da, which is in agreement with the

theoretical mass of 3283.240 Da (Table 1). As shown in Figure 4 and Figure S6 in the Supporting Information, cleavage of the His-His bond resulted in ions m/z 1511 and m/z 1773, indicating that the oxidized His residue is on the long chain highlighted in red. Moreover, the c2 and c3 ions from the short chain (highlighted in blue) together with the c2 to c5 ions from the long chain (highlighted in red) indicate the absence of modification for all residues N-terminal to His220 on both chains, thus ruling out cross-linking between Lys218 and His220. This is not unexpected, as at the pH for our studies, the amine on the lysine side chain is mostly protonated and thus renders it unreactive.[55,56] Also, of course, others factors such as local environment and solvation are known to modulate reactivities in enzymes and antibodies.[57−59] Taken together, our data have firmly established that the cross-linking is between the two heavy chain His220 residues.

Other Cross-Links. As reported in the literature,[9−11] cross-linking via thioether between the heavy chain hinge region and the light chain C-termini (HC:S215−K218/LC:T211−S218, S**C**DK/TVAPTE**C**S) was also observed in the photoirradiated IgG1 (Table S3 in the Supporting Information). The cleavage and formation of carbon−sulfur (C−S) bonds may occur via either homolytic (e.g., radical or photoinduced) or heterolytic (e.g, elimination and addition) mechanisms.[10,11,60,61] These additional cross-links may also account for the multiple nonreducible higher molecular species detected by SDS-PAGE and SEC described above (Figure S1 in the Supporting Information). In the SDS-PAGE gel (Figure S1 in the Supporting Information), the first band (with an apparent molecular weight about 92 kDa) for the sample pH9−3xLight (lane 10) was not observed in the samples pH4.8−3xLight (lane 8) and pH7−3xLight (lane 9). It is likely that this band corresponds to the thioether cross-link of LC-HC, as it is favorable under basic conditions.[9,10] Although the thioether cross-link between two heavy chains (e.g., Cys222-Cys222) has been reported after a higher dose of photo irradiation,[11] it was not detected in our sample by MS. The His-His cross-link of two heavy chains may contribute to the band with an apparent molecular weight about 100 kDa. The bands with apparent molecular weight about150 and 200 kDa are probably due to the cross-linking of more than two chains.

■ CONCLUSIONS

Our XChem-Finder workflow again leads to the discovery of an undefined and novel protein His-His cross-link, demonstrating its broad applicability and utility. Since the His-His cross-link is found in the highly conserved hinge region of IgG1, this modification most likely exists in other IgG1 molecules. As discussed above, a low level of cross-linking was present even without light stress, suggesting protein cross-linking in therapeutic proteins is perhaps more common than we have appreciated. Such drastic modification of proteins is likely to affect product quality, clinical efficacy, and even at low abundance, immunogenicity. Also again, to the best of our knowledge, there is no other alternative systematic approach that can be generally used to fully characterize protein cross-linking without *a priori* knowledge of the chemistry and site. With the rapid advancement in mass spectrometric techniques (e.g., high resolution and complementary fragmentation mechanisms), we expect the discovery and elucidation of other new protein cross-linking by our XChem-Finder approach will be equally successful.

■ AUTHOR INFORMATION

Corresponding Authors

*E-mail: mliu@amgen.com.
*E-mail: dren@amgen.com.
*E-mail: z.zhou@neu.edu.

Notes

The authors declare no competing financial interest.

■ REFERENCES

(1) Wilhelmus, M. M.; Grunberg, S. C.; Bol, J. G.; van Dam, A. M.; Hoozemans, J. J.; Rozemuller, A. J.; Drukarch, B. *Brain Pathol.* **2009**, *19*, 612–622.

(2) Wang, S. S.; Wu, J. W.; Yamamoto, S.; Liu, H. S. *Biotechnol. J.* **2008**, *3*, 165–192.

(3) Nemes, Z.; Devreese, B.; Steinert, P. M.; Van Beeumen, J.; Fesus, L. *FASEB J.* **2004**, *18*, 1135–1137.

(4) Balasubramanian, D.; Du, X.; Zigler, J. S., Jr. *Photochem. Photobiol.* **1990**, *52*, 761–768.

(5) Liu, H.; Gaza-Bulseco, G.; Faldu, D.; Chumsae, C.; Sun, J. *J. Pharm. Sci.* **2008**, *97*, 2426–2447.

(6) Beck, A.; Wagner-Rousset, E.; Ayoub, D.; Van Dorsselaer, A.; Sanglier-Cianferani, S. *Anal. Chem.* **2013**, *85*, 715–736.

(7) Lispi, M.; Datola, A.; Bierau, H.; Ceccarelli, D.; Crisci, C.; Minari, K.; Mendola, D.; Regine, A.; Ciampolillo, C.; Rossi, M.; Giartosio, C. E.; Pezzotti, A. R.; Musto, R.; Jone, C.; Chiarelli, F. *J. Pharm. Sci.* **2009**, *98*, 4511–4524.

(8) Liu, M.; Zhang, Z.; Zang, T.; Spahr, C.; Cheetham, J.; Ren, D.; Zhou, Z. S. *Anal. Chem.* **2013**, *85*, 5900–5908.

(9) Tous, G. I.; Wei, Z.; Feng, J.; Bilbulian, S.; Bowen, S.; Smith, J.; Strouse, R.; McGeehan, P.; Casas-Finet, J.; Schenerman, M. A. *Anal. Chem.* **2005**, *77*, 2675–2682.

(10) Cohen, S. L.; Price, C.; Vlasak, J. *J. Am. Chem. Soc.* **2007**, *129*, 6976–6977.

(11) Mozziconacci, O.; Kerwin, B. A.; Schoneich, C. *Chem. Res. Toxicol.* **2010**, *23*, 1310–1312.

(12) Wang, Z.; Rejtar, T.; Zhou, Z. S.; Karger, B. L. *Rapid Commun. Mass Spectrom.* **2010**, *24*, 267–275.

(13) Fujimori, E. *Invest. Ophthalmol. Vis. Sci.* **1982**, *22*, 402–405.

(14) Srivastava, O. P.; Kirk, M. C.; Srivastava, K. *J. Biol. Chem.* **2004**, *279*, 10901–10909.

(15) Lopez, B.; Gonzalez, A.; Hermida, N.; Valencia, F.; de Teresa, E.; Diez, J. *Am. J. Physiol. Heart Circ. Physiol.* **2010**, *299*, H1–H9.

(16) Shen, H. R.; Spikes, J. D.; Kopeckova, P.; Kopecek, J. *J. Photochem. Photobiol., B* **1996**, *35*, 213–219.

(17) Kroon, D. J.; Baldwin-Ferro, A.; Lalan, P. *Pharm. Res.* **1992**, *9*, 1386–1393.

(18) Van Buren, N.; Rehder, D.; Gadgil, H.; Matsumura, M.; Jacob, J. *J. Pharm. Sci.* **2009**, *98*, 3013–3030.

(19) Sinz, A. *Anal. Bioanal. Chem.* **2010**, *397*, 3433–3440.

(20) Petrotchenko, E. V.; Borchers, C. H. *Mass Spectrom Rev.* **2010**, *29*, 862–876.

(21) Walzthoeni, T.; Leitner, A.; Stengel, F.; Aebersold, R. *Curr. Opin. Struct. Biol.* **2013**, *23*, 252–260.

(22) Singh, P.; Panchaud, A.; Goodlett, D. R. *Anal. Chem.* **2010**, *82*, 2636–2642.

(23) Tang, X.; Bruce, J. E. *Methods Mol. Biol.* **2009**, *492*, 283–293.

(24) Bruce, J. E. *Proteomics* **2012**, *12*, 1565–1575.

(25) Singh, P.; Shaffer, S. A.; Scherl, A.; Holman, C.; Pfuetzner, R. A.; Larson Freeman, T. J.; Miller, S. I.; Hernandez, P.; Appel, R. D.; Goodlett, D. R. *Anal. Chem.* **2008**, *80*, 8799–8806.

(26) Wang, X.; Das, T. K.; Singh, S. K.; Kumar, S. *mAbs* **2009**, *1*, 254–267.

(27) Shen, H. R.; Spikes, J. D.; Kopecekova, P.; Kopecek, J. *J. Photochem. Photobiol., B* **1996**, *34*, 203–210.

(28) Agon, V. V.; Bubb, W. A.; Wright, A.; Hawkins, C. L.; Davies, M. J. *Free Radical Biol. Med.* **2006**, *40*, 698–710.

(29) Pattison, D. I.; Rahmanto, A. S.; Davies, M. J. *Photochem. Photobiol. Sci.: Off. J. Eur. Photochem. Assoc. Eur. Soc. Photobiol.* **2012**, *11*, 38–53.

(30) Liu, H.; Gaza-Bulseco, G.; Chumsae, C. *J. Am. Soc. Mass Spectrom.* **2009**, *20*, 2258–2264.

(31) Ren, D.; Pipes, G. D.; Liu, D.; Shih, L. Y.; Nichols, A. C.; Treuheit, M. J.; Brems, D. N.; Bondarenko, P. V. *Anal. Biochem.* **2009**, *392*, 12–21.

(32) Zhang, Z. *Anal. Chem.* **2011**, *83*, 8642–8651.

(33) Zhang, Z. *Anal. Chem.* **2004**, *76*, 3908–3922.

(34) Zhang, Z. *Anal. Chem.* **2010**, *82*, 1990–2005.

(35) Zhang, Z. *Anal. Chem.* **2005**, *77*, 6364–6373.

(36) Yao, X.; Freas, A.; Ramirez, J.; Demirev, P. A.; Fenselau, C. *Anal. Chem.* **2001**, *73*, 2836–2842.

(37) Yao, X.; Afonso, C.; Fenselau, C. *J. Proteome Res.* **2003**, *2*, 147–152.

(38) Gao, Q.; Xue, S.; Shaffer, S. A.; Doneanu, C. E.; Goodlett, D. R.; Nelson, S. D. *Eur. J. Mass Spectrom.* **2008**, *14*, 275–280.

(39) Gao, Q.; Xue, S.; Doneanu, C. E.; Shaffer, S. A.; Goodlett, D. R.; Nelson, S. D. *Anal. Chem.* **2006**, *78*, 2145–2149.

(40) Back, J. W.; Notenboom, V.; de Koning, L. J.; Muijsers, A. O.; Sixma, T. K.; de Koster, C. G.; de Jong, L. *Anal. Chem.* **2002**, *74*, 4417–4422.

(41) Liu, M.; Cheetham, J.; Cauchon, N.; Ostovic, J.; Ni, W.; Ren, D.; Zhou, Z. S. *Anal. Chem.* **2012**, *84*, 1056–1062.

(42) Wan, W.; Zhao, G.; Al-Saad, K.; Siems, W. F.; Zhou, Z. S. *Rapid Commun. Mass Spectrom.* **2004**, *18*, 319–324.

(43) Swaney, D. L.; Wenger, C. D.; Coon, J. J. *J. Proteome Res.* **2010**, *9*, 1323–1329.

(44) Ni, W.; Lin, M.; Salinas, P.; Savickas, P.; Wu, S. L.; Karger, B. L. *J. Am. Soc. Mass Spectrom.* **2013**, *24*, 125–133.

(45) Ingrosso, D.; Fowler, A. V.; Bleibaum, J.; Clarke, S. *Biochem. Biophys. Res. Commun.* **1989**, *162*, 1528–1534.

(46) Tetaz, T.; Morrison, J. R.; Andreou, J.; Fidge, N. H. *Biochem Int.* **1990**, *22*, 561–566.

(47) Ni, W.; Dai, S.; Karger, B. L.; Zhou, Z. S. *Anal. Chem.* **2010**, *82*, 7485–7491.

(48) Sorensen, S. B.; Sorensen, T. L.; Breddam, K. *FEBS Lett.* **1991**, *294*, 195–197.

(49) Kim, M. S.; Pandey, A. *Proteomics* **2012**, *12*, 530–542.

(50) Syka, J. E.; Coon, J. J.; Schroeder, M. J.; Shabanowitz, J.; Hunt, D. F. *Proc. Natl. Acad. Sci. U.S.A.* **2004**, *101*, 9528–9533.

(51) Tomita, M.; Irie, M.; Ukita, T. *Biochemistry* **1969**, *8*, 5149–5160.

(52) Kang, P.; Foote, C. S. *J. Am. Chem. Soc.* **2002**, *124*, 9629–9638.

(53) Nilsson, R.; Merkel, P. B.; Kearns, D. R. *Photochem. Photobiol.* **1972**, *16*, 117–124.

(54) Verweij, H.; Dubbelman, T. M.; Van Steveninck, J. *Biochim. Biophys. Acta* **1981**, *647*, 87–94.

(55) Alfaro, J. F.; Gillies, L. A.; Sun, H. G.; Dai, S.; Zang, T.; Klaene, J. J.; Kim, B. J.; Lowenson, J. D.; Clarke, S. G.; Karger, B. L.; Zhou, Z. S. *Anal. Chem.* **2008**, *80*, 3882–3889.

(56) Zang, T.; Dai, S.; Chen, D.; Lee, B. W.; Liu, S.; Karger, B. L.; Zhou, Z. S. *Anal. Chem.* **2009**, *81*, 9065–9071.

(57) Zhou, Z. S.; Flohr, A.; Hilvert, D. *J. Org. Chem.* **1999**, *64*, 8334−8341.

(58) Zhao, G.; Zhou, Z. S. *Bioorg. Med. Chem. Lett.* **2001**, *11*, 2331−2335.

(59) Zhou, Z. S.; Jiang, N.; Hilvert, D. *J. Am. Chem. Soc.* **1997**, *119*, 3623−3624.

(60) Zhou, Z. S.; Smith, A. E.; Matthews, R. G. *Bioorg. Med. Chem. Lett.* **2000**, *10*, 2471−2475.

(61) Matthews, R. G.; Smith, A. E.; Zhou, Z. S.; Taurog, R. E.; Bandarian, V.; Evans, J. C.; Ludwig, M. *Helv. Chim. Acta* **2003**, *86*, 3939−3954.